

# Low-temperature sintering of MnO<sub>2</sub>-doped PZT–PZN Piezoelectric ceramics

Sung-Mi Lee · Seung-Ho Lee · Chang-Bun Yoon ·  
Hyoun-Ee Kim · Kyung-Woo Lee

Received: 14 May 2006 / Revised: 11 April 2007 / Accepted: 9 May 2007 / Published online: 23 May 2007  
© Springer Science + Business Media, LLC 2007

**Abstract** The effect of MnO<sub>2</sub> addition on the microstructural evolution and piezoelectric properties of low temperature sinterable PZT–PZN ceramics was investigated. When a small amount of MnO<sub>2</sub> ( $\leq 0.5$  wt%) was added, the Mn ions were homogeneously dissolved in the PZT–PZN ceramics, leading to full densification at a temperature as low as 930 °C. However, the further addition of MnO<sub>2</sub> hindered the densification, causing the specimen to have a high porosity and small grain size. In addition, as the MnO<sub>2</sub> content increased, the crystal structure of the PZT–PZN changed gradually from a tetragonal to a rhombohedral phase, due to the substitution of Mn for the B-sites in the perovskite structure. The addition of MnO<sub>2</sub> up to a maximum of 0.5% improved the mechanical quality factor ( $Q_m$ ) of the PZT–PZN ceramics markedly, while keeping the  $k_p$  and  $d_{33}$  values reasonably high. The 80% PZT–20% PZN doped with 0.4 wt% MnO<sub>2</sub> exhibited excellent piezoelectric properties;  $Q_m=1,000$ ,  $k_p=0.62$ , and  $d_{33}=330$  pC/N.

**Keywords** Piezoelectric ceramics · Donor doping · Piezoelectric properties · Mechanical quality factor

## 1 Introduction

Lead zirconate titanate (PZT) ceramics have been widely used as actuators, resonators, transducers, and transformers, because of their excellent piezoelectric properties [1]. To broaden the range of applications of these ceramics, it is necessary to lower their sintering temperature, because this allows them to be co-fired with less expensive electrode materials (e.g., Ag) for multilayer devices [2, 3].

A number of methods of decreasing the sintering temperature of PZT ceramics have been reported, including the fine-powder approach, hot-pressing, and the addition of low-temperature meltable additives [4–6]. However, while these methods all have their advantages, they also have certain disadvantages. For example, the fine-powder approach using chemical procedures is quite complex and difficult to control, while the addition of low-temperature meltable additives generally deteriorates the piezoelectric properties.

Previously, we developed a new approach to the sintering of PZT-based ceramics at temperatures as low as 900 °C, by adding lead zinc niobate (PZN) relaxor material [7, 8]. The resultant low-temperature sintered PZT–PZN ceramics exhibited excellent piezoelectric properties, with the parameters:  $d_{33}=500$  pC/N,  $k_p=0.68$ , and  $S_{33}=0.38\%$  at 2 kV/mm. These PZT–PZN ceramics enabled us to fabricate various actuators [3] and motors [9] with high performances by co-firing them with silver electrodes.

However, the mechanical quality factor ( $Q_m$ ) of these materials was too low for them to be used as transformers or certain types of actuators. In such cases, a high  $Q_m$  value is a prerequisite, because the mechanical vibration at the resonance frequency plays an important role in these applications. The  $Q_m$  of the PZT–PZN ceramics might be enhanced by traditional approaches, such as the substitution

S.-M. Lee · S.-H. Lee · C.-B. Yoon · H.-E. Kim (✉)  
School of Materials Science and Engineering,  
Seoul National University,  
Seoul 151-742, South Korea  
e-mail: kimhe@snu.ac.kr

K.-W. Lee  
Kyungwon Ferrite Ind. Co., LTD,  
1260-4 Chungwang-dong,  
Shiheung-si, Kyonggi-do 429-450, South Korea

of the ions at the B-sites of the perovskite structure [10]. Several researchers have successfully improved the  $Q_m$  of PZT-based ceramics by adding Mn-containing compounds, because Mn ions are homogeneously dissolved in the perovskite structure and act as acceptors [11–18]. In this study, we investigated the effect of  $MnO_2$  addition on the sinterability, crystal structures, and piezoelectric properties (i.e.,  $Q_m$ ,  $k_p$ ,  $d_{33}$ ) of PZT–PZN sintered at 930 °C.

## 2 Experimental procedure

Based on our previous studies, three PZT–PZN compositions were selected; 90% PZT(51/49)–10% PZN, 80% PZT(50/50)–20% PZN, and 70% PZT(48/52)–30% PZN [7]. These are all MPB compositions and the numbers in parenthesis indicate the Zr/Ti ratios. The amount of  $MnO_2$  added to the PZT–PZN ceramics was increased from 0 to 1 wt% in increments of 0.1 wt%.

The PZT–PZN powders were prepared using high-purity  $PbO$ ,  $ZnO$ ,  $Nb_2O_5$ ,  $ZrO_2$ , and  $TiO_2$  powders. (all 99.9% purity, Aldrich Chem. Co, Milwaukee, WI, USA). The powders were weighed and mixed together by ball-milling with zirconia balls as the media in ethyl alcohol. The resultant mixture was dried and then calcined in an alumina crucible at 850 °C for 4 h, producing the PZT–PZN phase. Thereafter, predetermined amounts of  $MnO_2$  powder (99% purity, Aldrich Chem. Co) were mixed with the calcined PZT–PZN powder by ball-milling for 48 h. The mixture was then dried and sieved to form fine powders.

The green samples with a diameter of 15 mm and thickness of 1 mm were fabricated by dry-pressing, followed by cold isostatic pressing at 200 MPa. The specimens were sintered at 930 °C for 4 h in a sealed alumina crucible with a  $PbZrO_3$  atmosphere engendered by the presence of  $PbZrO_3$  powder. The densities of the specimen were measured by the Archimedes method. The microstructural evolution was observed using a scanning electron microscope (SEM; Model JSM-5600, JEOL Technics, Tokyo, Japan). The crystal structure after sintering was examined using X-ray diffractometry (XRD: Model MXP18A-HF, MAC Science, Tokyo, Japan) with a  $2\theta$  angle ranging from 20 to 60°.

In order to measure the piezoelectric properties of the PZT–PZN ceramics doped with  $MnO_2$ , the sintered disks were lapped and electroded with a silver paste. The specimens were poled in a silicone oil bath at 200 °C by applying an electric field of 2 kV/mm for 20 min. The specimens were aged for 24 h prior to testing. The piezoelectric constant ( $d_{33}$ ) was measured using a quasi-static piezoelectric  $d_{33}$ -meter (Model ZJ-3D, Institute of Acoustics Academic Sinica, Beijing, China). The electro-mechanical coupling coefficient ( $k_p$ ) and mechanical quality

factor ( $Q_m$ ) were determined by the resonance-antiresonance technique using an impedance analyzer (Model HP4194A, Hewlett-Packard, Palo Alto, CA). The dielectric properties were measured as a function of the temperature using an impedance analyzer (SI1260 Impedance/Gain-phase Analyzer, Solatron, UK).

## 3 Results and discussion

The addition of  $MnO_2$  had a significant influence on the density, microstructure and crystal structure of the PZT–PZN system. The density of the 0.8 PZT–0.2 PZN sample sintered at 930 °C for 4 h in air as a function of the  $MnO_2$  content is shown in Fig. 1. For  $MnO_2$  contents of up to 0.5 wt%, the samples were almost fully dense. However, when the  $MnO_2$  content exceeded 0.5 wt%, the density decreased rapidly.

The effect of  $MnO_2$  addition on the density was also clearly visible in the SEM micrographs, as shown in Fig. 2(a)–(d). The fracture surface of the pure PZT–PZN sample revealed almost full densification with an average grain size of  $\sim 2 \mu m$  (Fig. 2(a)). This good densification was maintained until the  $MnO_2$  content was increased up to 0.5 wt% and, within this range, the grain size increased slightly with increasing  $MnO_2$  content, reflecting the enhanced mobility of the constituent ions for grain growth (Fig. 2(b)). On the other hand, when more than 0.5 wt%  $MnO_2$  was added, some pores were formed at the grain boundary (Fig. 2(c)). This retarded densification became more serious with further addition of  $MnO_2$ . For instance, when 0.8 wt%  $MnO_2$  was added, the sample was barely sintered, as shown in Fig. 2(d). These results are in good agreement with the measured densities of the specimens.

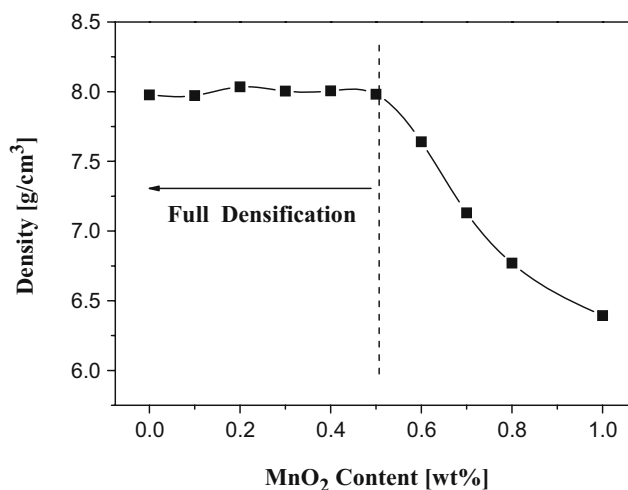
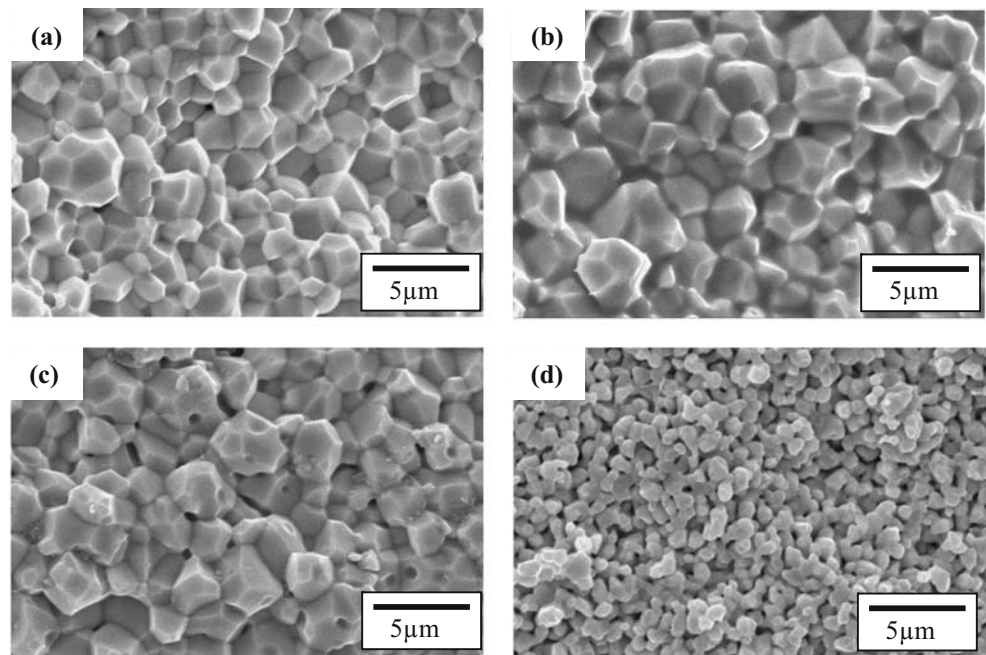


**Fig. 1** Density of the 0.2 PZN–0.8 PZT specimens sintered at 930 °C as a function of the  $MnO_2$  content

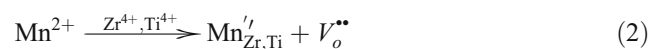
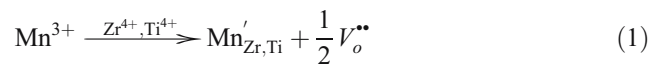
**Fig. 2** SEM microstructures of the fracture surfaces of the 0.2 PZN–0.8 PZT specimens with MnO<sub>2</sub> added: (a) 0 wt%, (b) 0.4 wt%, (c) 0.6 wt%, and (d) 0.8 wt%



Similar results were observed for the other two compositions, namely 0.9 PZT–0.1 PZN and 0.7 PZT–0.3 PZN. However, the range of MnO<sub>2</sub> content which allowed for full densification was dependent on the PZN content, as shown in Fig. 3. As the PZN content was increased, the amount of MnO<sub>2</sub> that could be incorporated without hindering the densification was increased.

It is well known that when MnO<sub>2</sub> is added to PZT-based ceramics without exceeding the solubility limit, the Mn ions are homogeneously dissolved in the perovskite structure, thereby enhancing the densification of the sample. More specifically, the B-site ions in the perovskite structure (Zr<sup>4+</sup>,

Ti<sup>4+</sup>) are substituted with the Mn ions which have lower valences (Mn<sup>2+</sup> or Mn<sup>3+</sup>), creating oxygen vacancies as follows:



The Mn ion is thermodynamically most stable in the valence state of 3 in the sintering temperature range used

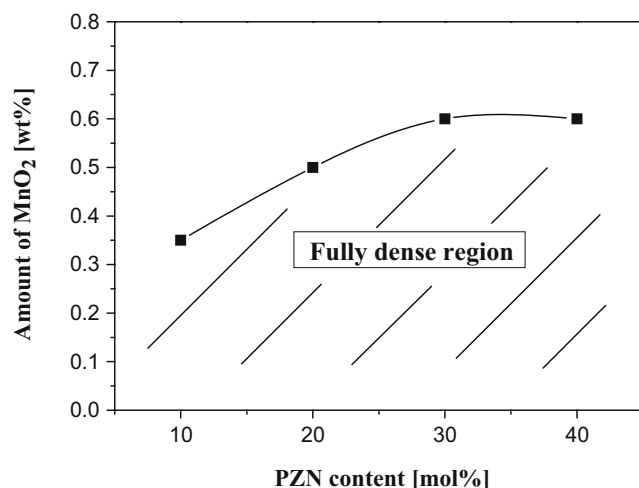


**Fig. 3** Densification limit of MnO<sub>2</sub> in PZT–PZN ceramic at 930 °C as a function of the PZN content

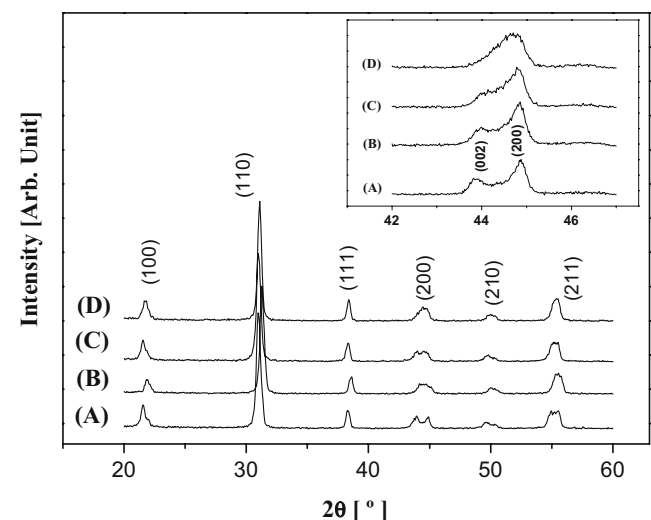


**Fig. 4** X-ray diffraction pattern of the 0.2 PZN–0.8 PZT specimens with different amounts of MnO<sub>2</sub>: A, 0 wt%; B, 0.4 wt%; C, 0.6 wt%, and D, 0.8 wt%

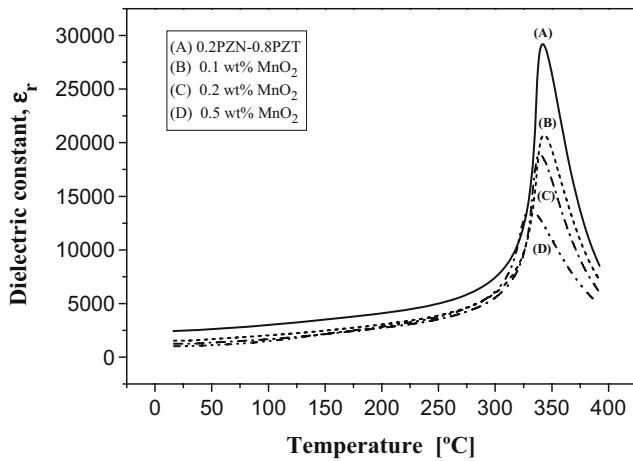


**Fig. 5** Relative dielectric constant ( $\epsilon_r$ ) of the PZT–PZN specimens as a function of the  $\text{MnO}_2$  content

in this study [19]. Therefore, the reaction in Eq. 1 is favored over that in Eq. 2. In the present PZN–PZT system, in addition to Zr or Ti,  $\text{Mn}^{3+}$  ions can substitute for the  $\text{Nb}^{5+}$  ions at the B-sites as follows;



In this case, a larger number of vacant oxygen sites are created than in the case of pure PZT. The increase in the densification limit of  $\text{MnO}_2$  with increasing PZN content (Fig. 3) was attributed to this behavior.

There were no traces of pyrochlore phase or impurities in the XRD patterns of any of the specimens, as shown in Fig. 4, (A)–(D). However, the addition of  $\text{MnO}_2$  changed the crystal structure of the samples. Pure 0.8 PZT–0.2 PZN without  $\text{MnO}_2$  had a tetragonal structure, as evidenced by

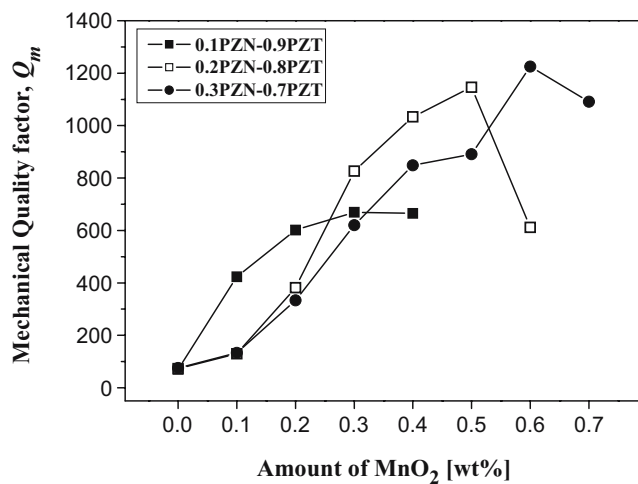


**Fig. 6** Mechanical quality factor ( $Q_m$ ) of the PZT–PZN specimens as a function of the  $\text{MnO}_2$  content

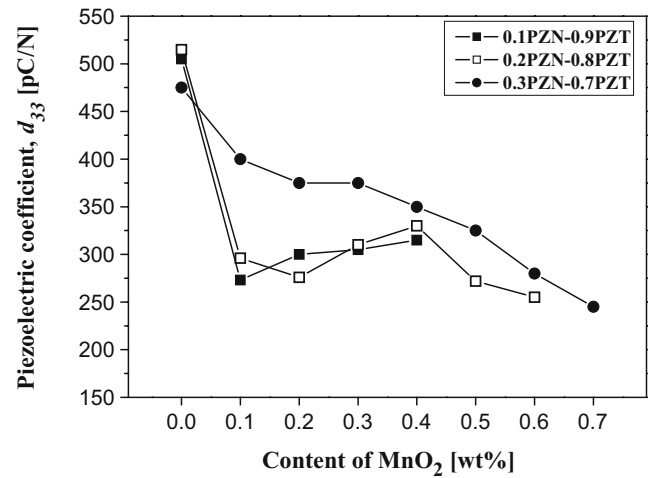


**Fig. 7** Piezoelectric coefficient ( $d_{33}$ ) of the PZT–PZN specimens as a function of the  $\text{MnO}_2$  content

the splitting of the (002) and (200) peaks (Fig. 4, (A)). With increasing  $\text{MnO}_2$  content, the perovskite structure gradually changed from a tetragonal to a rhombohedral structure, as shown in Fig. 4, (B)–(D). This change in the crystal structure is deemed to be related to the substitution of the Mn ions for the B-site ions in the perovskite structure, as is often the case with Mn-doped PZT-based ceramics [20].

The observed changes in the densification, microstructure, and crystal structure of the PZT–PZN ceramics caused by the addition of  $\text{MnO}_2$  strongly affected their electrical properties. Figure 5 shows the relative dielectric constant ( $\epsilon_r$ ) of the PZT–PZN ceramic as a function of the amount of  $\text{MnO}_2$ . It was observed that the addition of  $\text{MnO}_2$  led to the steady drop in the  $\epsilon_r$  value. As the  $\text{MnO}_2$  content increased from 0 to 0.5 wt%, the  $\epsilon_r$  value decreased from 2,400 to 1,000. On the other hand, all of the fabricated samples

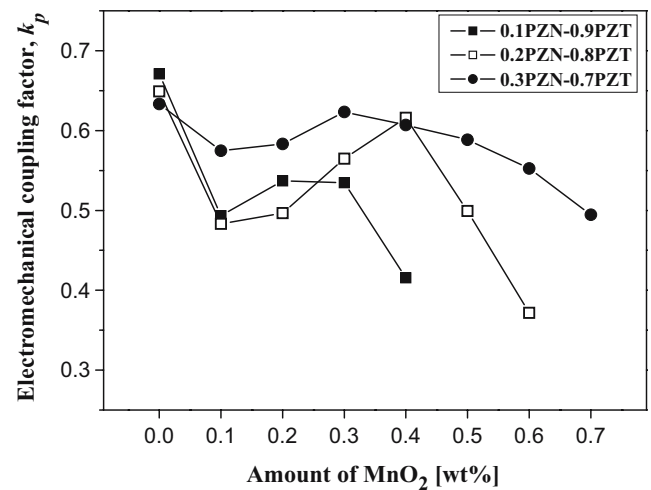


**Fig. 8** Electromechanical coupling factor ( $k_p$ ) of the PZT–PZN specimens as a function of the  $\text{MnO}_2$  content

showed relatively high Curie temperatures of higher than 325 °C, regardless of the MnO<sub>2</sub> content. Only a slight decrease in  $T_c$  was observed with increasing MnO<sub>2</sub> content.

The piezoelectric properties of the PZT–PZN were much influenced by the MnO<sub>2</sub> additions. The mechanical quality factor ( $Q_m$ ) of the PZT–PZN ceramics doped with MnO<sub>2</sub> was markedly improved, as shown in Fig. 6. As the MnO<sub>2</sub> content in the 0.8 PZT–0.2 PZN ceramics was increased up to 0.5 wt%, the  $Q_m$  value increased steadily up to ~1,200, because the Mn ions at the (Ti, Zr) sites in the lattice acted as acceptors. More specifically, the substitution of Mn ions in the B-sites of the perovskite structure increases the number of oxygen vacancies. These oxygen vacancies induce a space charge and internal field inside the PZT grains, which inhibits the motion of the domain, thereby increasing the  $Q_m$  value [21]. However, when the MnO<sub>2</sub> content exceeded a certain threshold value (>0.5 wt%), the  $Q_m$  value decreased, apparently due to insufficient densification.

The piezoelectric coefficient ( $d_{33}$ ) of the PZT–PZN ceramics is shown in Fig. 7 as a function of the MnO<sub>2</sub> content. The pure 0.9 PZT–0.1 PZN and 0.8 PZT–0.2 PZN samples without MnO<sub>2</sub> showed  $d_{33}$  values of around 500 pC/N. When a small amount of MnO<sub>2</sub> (0.1 wt%) was added, the  $d_{33}$  value decreased rapidly to approximately 300 pC/N. It is believed that the Mn ions act as acceptors so as to create oxygen vacancies, which inhibit the movement of the ferroelectric domain walls, thereby leading to a decrease in the  $d_{33}$  value. With the further addition of MnO<sub>2</sub>, the  $d_{33}$  remained constant, presumably due to the compensating effects of acceptor doping and grain growth [22]. On the other hand, the  $d_{33}$  value of the 0.7 PZT–0.3 PZN sample decreased steadily with increasing MnO<sub>2</sub> content, suggesting that the grain growth effect is dominant over the acceptor effect in this system.

The electromechanical coupling factor ( $k_p$ ) of PZT–PZN exhibited similar behavior to that of the  $d_{33}$  value with the addition of MnO<sub>2</sub>, as shown in Fig. 8. With increasing MnO<sub>2</sub> content, the  $k_p$  value at first decreased and then remained constant or even increased slightly. This initial rapid decrease in the value of  $k_p$  is attributed to the acceptor effect. The increase in the grain size with increasing MnO<sub>2</sub> content has the effect of limiting the decrease in the value of  $k_p$ , causing it to bottom out. These results on the piezoelectric properties proved that the addition of MnO<sub>2</sub> to PZT–PZN ceramics remarkably increases the  $Q_m$  value, while keeping the  $k_p$  and  $d_{33}$  values reasonably high, as compared to those of the pure PZT–PZN ceramics. This improvement in  $Q_m$  value would make the MnO<sub>2</sub> doped PZT–PZN ceramics to be used for wider applications, such as transformers or certain types of actuators.

#### 4 Summary and conclusion

The electromechanical quality factor ( $Q_m$ ) of the PZT–PZN system was markedly enhanced by the addition of small amounts of MnO<sub>2</sub>. With the addition of less than 0.5 wt% of MnO<sub>2</sub>, the PZT–PZN was fully dense when sintered at 930 °C for 4 h in air. With increasing MnO<sub>2</sub> content up to maximum of 0.5 wt%, the grain size of the specimen increased and the crystal structure changed from tetragonal to rhombohedral. When 0.4 wt% MnO<sub>2</sub> was added to the PZT–PZN system, the  $Q_m$  value exceeded 1,000, while the  $k_p$  and  $d_{33}$  values remained above 0.6 and 300 pC/N, respectively.

#### References

1. B. Jaffe, W.R. Cook, H. Jaffe, *Piezoelectric Ceramics*. (Academic, London, UK, 1971).
2. C.B. Yoon, S.H. Lee, S.M. Lee, H.E. Kim, *J. Am. Ceram. Soc.* **87**, 1663 (2004)
3. C.B. Yoon, S.M. Lee, S.H. Lee, H.E. Kim, *Sens. Actuators A. A* **119**, 221 (2005)
4. T. Hayashi, T. Inoue, Y. Akiyama, *J. Eur. Ceram. Soc.* **19**, 999 (1999)
5. N.D. Patel, P.S. Nicholson, *Am. Ceram. Soc. Bull.* **65**, 783 (1986)
6. K. Murakami, D. Mabuchi, T. Kurita, Y. Niwa, S. Kaneko, *Jpn. J. Appl. Phys.* **35**, 5188 (1996)
7. S.M. Lee, C.B. Yoon, S.H. Lee, H.E. Kim, *J. Mater. Res.* **19**, 2553 (2004)
8. S.B. Seo, S.H. Lee, C.B. Yoon, G.T. Park, H.E. Kim, *J. Am. Ceram. Soc.* **87**, 1238 (2004)
9. C.B. Yoon, G.T. Park, H.E. Kim, J.H. Ryu, *Sens. Actuators A. A* **121**, 515 (2005)
10. S.H. Lee, C.B. Yoon, S.B. Seo, H.E. Kim, *J. Mater. Res.* **40**, 1765 (2003)
11. J.S. Kim, K.H. Yoon, J.O. Park, J.M. Lee, *J. Korean Ceram. Soc.* **27**, 187 (1990)
12. J.H. Moon, H.M. Jang, *J. Mater. Res.* **8**, 3184 (1993)
13. Y. Hou, M. Zhu, F. Gao, B. Wang, C. Tian, *J. Am. Ceram. Soc.* **87**, 847 (2004)
14. K.H. Yoon, H.K. Lee, H.R. Lee, *J. Am. Ceram. Soc.* **85**, 2753 (2002)
15. S.J. Yoon, A. Joshi, K. Uchino, *J. Am. Ceram. Soc.* **80**, 1035 (1997)
16. S.J. Yoon, S.J. Yoo, J.H. Moon, J.H. Jung, H.J. Kim, *J. Mat. Res.*, **11**, 348 (1996)
17. A.P. Barranco, F.C. Pinar, P. Martinez, E.T. Garcia, *J. Eur. Ceram. Soc.*, **21**, 523 (2001)
18. J.H. Park, J. Park, J.G. Park, B.K. Kim, Y. Kim, *J. Eur. Ceram. Soc.*, **21**, 1383 (2001)
19. *CRC Handbook of Chemistry and Physics*. (CRC, Boca Raton, FL, 1985)
20. L.X. He, C.E. Li, *J. Mater. Sci.*, **35**, 2477 (2000)
21. Y.H. Xu, *Ferroelectric Materials and Their Application*. (Elsevier, Amsterdam, The Netherlands, 1991)
22. C.A. Randall, N. Kim, J.P. Kucera, W. Cao, T.R. Shrout, *J. Am. Ceram. Soc.* **81**, 677 (1998)